

# Towards detecting the pathological subharmonic voicing with fully convolutional neural networks

Takeshi Ikuma *Member, IEEE*, Melda Kunduk, Brad Story, and Andrew J. McWhorter

**Abstract**—Many voice disorders induce subharmonic phonation, but voice signal analysis is currently lacking a technique to detect the presence of subharmonics reliably. Distinguishing subharmonic phonation from normal phonation is a challenging task as both are nearly periodic phenomena. Subharmonic phonation adds cyclical variations to the normal glottal cycles. Hence, the estimation of subharmonic period requires a wholistic analysis of the signals. Deep learning is an effective solution to this type of complex problem. This paper describes fully convolutional neural networks which are trained with synthesized subharmonic voice signals to classify the subharmonic periods. Synthetic evaluation shows over 98% classification accuracy, and assessment of sustained vowel recordings demonstrates encouraging outcomes as well as the areas for future improvements.

**Index Terms**—Disordered voice, Acoustic voice analysis, Deep learning

## I. INTRODUCTION

Subharmonic phonation is a voicing mode in which the vibration pattern of vocal folds varies from cycle to cycle before repeating itself. It is often associated with vocal pathology, especially those which alter the physical characteristics of the vocal folds such as vocal fold lesions and vocal fold paralysis [1, 2, 3, 4, 5]. Subharmonic voicing is also possible for vocally healthy speakers. Subharmonics can be voluntarily produced as vocal fry [6] or as a singing technique [7]. Perceptually, the subharmonic voice presents rough voice quality [8] or lowered pitch [9, 10, 11].

The presence of subharmonics may degrade the accuracy of the voice parameter measurements used in clinical acoustic analysis. This stems from the primary property of the subharmonic signals, that is, they are nearly periodic as is the normal phonation. This similarity often causes existing fundamental frequency estimators to yield erroneous estimates under strong subharmonics [12, 13]. The (speaking) fundamental frequency  $f_o$  that those algorithms estimates is the foundation of the most of voice parameters and should represent the cycle frequency of glottal opening and closing, disregarding the variabilities in cyclic variations in amplitude, frequency, or shape. Incorrectly

using the subharmonic fundamental frequency (e.g.  $f_o/2$  for period doubling subharmonics) as the  $f_o$  likely results in the final parameter measures to under-represent the severity of pathological voice. As such, an accurate numerical solution to detect the presence of the subharmonics is important for the pathological voice analysis.

Titze [14] in 1994 categorized voice signals which encompass the subharmonic behaviors as type 2 in his voice signal typing system. His recommended approach to analyze type 2 signals is by visualization tools and subjective inspection and discouraged the use of numerical measures citing their unreliability. Since 1994, little success has been reported to analyze subharmonic voice signals. The NSH (number of subharmonics) parameter of KayPENTAX MDVP software [15, 16] reportedly has a poor accuracy [2]. Sun [17] introduced the concept of the subharmonic-to-harmonic ratio (SHR) and used it to estimate the fundamental frequency of voice signals with a possible presence of period-doubling subharmonics, and Hlavnička et al. [18] strengthened Sun’s method with improved initial  $f_o$  estimation. Sun’s approach, however, is not the ideal solution to compute the SHR as there is a conundrum of trying to measure the SHR without knowing the presence of the subharmonics. These methods are also limited to detect period-doubling subharmonics and not higher-period subharmonics that are also prevalent in pathological voice [5]. Aichinger et al. [19] proposed to use two harmonic models to analyze biphonic voice (i.e., two parts of glottis vibrating at different frequencies) but a strong coupling of the two sources, which induces subharmonics, causes the analysis to fail [20]. Finally, Awan and Awan [21] proposed two-stage cepstrum peak prominence difference to measure vocal roughness. While this parameter was derived to measure the difference between the  $f_o$  and the subharmonic (or true) fundamental frequency, it requires the approximate range of the expected  $f_o$ , and it reportedly failed to report subharmonics sufficiently [22].

Accurate detection of incidental subharmonics over a short segment of voice signal leads to improve the subharmonic measures such as NSH and SHR and to aid the  $f_o$  estimation, thereby also improving the qualities of the vocal parameters at large. Detection of subharmonics is synonymous to estimation of the subharmonic period  $M$ , noting that  $M = 1$  naturally lend itself to the normal phonation. This paper explores deep learning (DL) as a potential solution to classify the subharmonic period. This idea is motivated by the DL fundamental frequency estimators [23, 24]. These estimators outperform the conventional estimators and demonstrated their robustness against the presence of subharmonics [12]. If a DL network

T. Ikuma is with Department of Otolaryngology–Head and Neck Surgery, Louisiana State University Health Sciences Center, New Orleans, LA.

M. Kunduk is with Department of Communication Disorders, Louisiana State University, Baton Rouge, LA.

B. Story is with Dept. of Speech, Language, Hearing Sciences, University of Arizona.

A. J. McWhorter is with Department of Otolaryngology–Head and Neck Surgery, Louisiana State University Health Sciences Center, New Orleans, LA.

This manuscript is an extended version of an abstract submitted to the 16th International Conference on Advances in Quantitative Laryngology, Voice and Speech Research, Groningen, the Netherlands, June 24th - 27th, 2025.

can be trained to ignore subharmonics, a similar network could likely be trained to find subharmonics. We specifically investigate the efficacy of fully convolutional neural network (FCN) architecture.

The rest of paper is organized as follows. Section II defines the DL networks under study and Section III establishes the subharmonic signal synthesis framework used to train and evaluate the networks. The performance of the trained networks is presented with the synthesized signals in Section IV and with real sustained vowel recordings in Section V, followed by the concluding remarks.

## II. FULLY CONVOLUTIONAL NEURAL NETWORKS

Clinical voice recordings have arbitrary durations, and this makes the fully convolutional neural network (FCN) architecture [25, 26, 27] a suitable DL model as is used for the  $f_o$  estimation [23]. Time-varying nature of voice signals requires most of their analysis parameters to be computed over a short sliding window, and the subharmonic period is no different as subharmonic voicing in pathological voice can occur intermittently and possibly in a rapid succession [1, 5, 14, 28]. FCN with local pooling layers is fit to perform this task efficiently with overlapping snapshots as a pooling layer acts as a generalized downsampler, thus decoupling the window size and the snapshot interval.

The input sampling rate  $f_s$  is set to 8000 samples per second (S/s), which is sufficient to estimate the vocal fundamental frequency ( $f_o$ ) [23], and thus also sufficient for subharmonic period. Two FCNs are evaluated with different target window sizes: 400 samples (50 ms) and 800 samples (100 ms). The shorter window is designed to be more robust against intermittency while the longer window aims to improve the classification performance of sustained subharmonics. The output interval is set to 2 ms or 500 samples/second, requiring the pooling layers collectively to reduce the sampling rate by 8.

The subharmonic period  $M$  can theoretically be any positive integer; however, the vast majority is period doubling ( $M = 2$ ) and the prevalence rapidly diminishes as  $M$  increases [5, 12, 18]. Also, a signal snapshot must contain more than  $M + 1$  glottal cycles for the classifier to determine the subharmonic period  $M$  with any confidence. The maximum  $M$  is set to four with the label set  $\mathcal{M} = \{1, 2, 3, 4\}$ , based on the target window sizes and expected range of  $f_o$  (100-300 Hz).

The FCN structure under study comprises 5 convolutional layers as depicted in Fig. 1. The input signal  $x_n$  is a pre-normalized acoustic signal of arbitrary duration, and the first 4 convolutional layers are accompanied by max pooling two consecutive samples, each effectively downsampling the propagating signal by 2 and collectively by 8. These convolutional layers are also followed by batch normalization and rectified linear unit (ReLU) activation function. The final output convolutional layer has four channels to sigmoid activation functions. The network outputs  $\{P_{M,k} : M \in \mathcal{M}\}$ , the probabilities of the  $k$ th snapshot contains the signal with subharmonic period  $M$ . The softmax activation is not used at the output because the subharmonic period candidates in

$\mathcal{M}$  is not exhaustive set of pathological voice signals. The number of filters and their sizes of each convolution layer are denoted in Fig. 1. The same network architecture is used for both of the target window sizes by using different allocations of its coefficients for the fourth convolution layer. The first network, named FCN-401, with 401-sample (50.1-ms) window size uses many short filters (512 filters of 16-coefficient filters) while the second network, FCN-785 with 785-sample (98.1-ms) window size with a few long filter (128 length-64 filters). Thus, both networks have the same number of coefficients and incur nearly the same computational complexity.

## III. SYNTHESIS OF TRAINING DATASET

For the DL training and evaluation, having a dataset with known truths is essential. Clinical voice recordings require manual annotation, and the accuracy of manual annotation is questionable because of the nearly periodic nature of subharmonic signals. Hence, we turned to a numerical voice synthesis model to parameterize the subharmonic voicing and generate a large dataset via Monte Carlo simulation.

To study the subharmonic phonation, prior work in literature also utilized synthesis tools to generate voice signals with subharmonics [9, 18, 29, 11]. These studies were all based on introducing amplitude or frequency modulation to the source glottal flow signal via cycle-wise manipulation of the signal and were limited to period-doubling subharmonics. This general approach limits the complexity of the generated signals because the flow pulse shapes are merely time- or amplitude-scaled versions.

In this study, the synthesis process employed the kinematic vocal fold model [30, 31], which was aerodynamically and acoustically coupled to two-port wave propagation vocal tract model [32, 33]. This synthesis framework was previously used to study breathy voice [34, 35] and vocal fold asymmetry [36]. The kinematic model was also used to simulate the period-doubling electroglottographic (EGG) signals although the subharmonics were introduced post-synthesis [29]. In the current work, the subharmonic modulation is introduced to the vocal fold vibration so that the modulation is subject to the vocal fold collision and the nonlinear relationship between the glottal area and glottal flow. This approach realizes a more diverse set of subharmonics than previous synthesis approaches and naturally extends to the generation of higher-period subharmonics.

The kinematic vocal fold model [30, 31] is built around a three-dimensional geometry of symmetric vocal folds. In exchange for removing the displacement-force coupling of mass-spring models [37, 38], the kinematic model concretely defines the movements of the vocal folds. This enables simple and direct incorporation of subharmonic vibration to the model. The displacement function without the presence of the other vocal fold is modeled by

$$\tilde{\xi}(y, z, t) = \xi_0(y, z) + \xi_m \sin(\pi y/L)r(t; \varphi), \quad (1)$$

where  $L$  is the vibrating glottal length,  $T$  is the vibrating glottal thickness,  $\xi_0(y, z)$  is the prephonatory edge position,

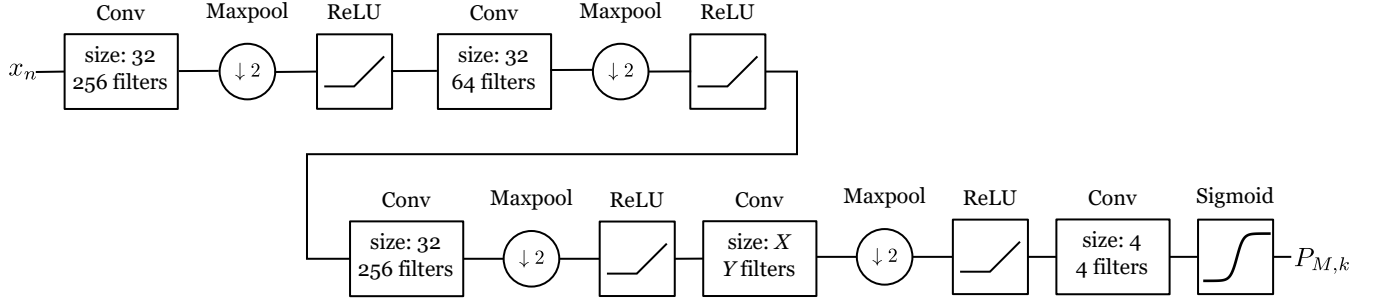


Fig. 1: Fully convolutional neural network architecture under study: FCN-401 with  $X = 16$  and  $Y = 512$ , and FCN-785 with  $X = 64$  and  $Y = 128$ . All convolutional layers are applied with a stride of 1, and there is a batch normalization layer (not pictured) before every ReLU.

$\xi_m$  is the maximum vocal fold displacement,  $r(t; \varphi)$  is the reference vibration function, and

$$\varphi = -2\pi Q_p(z/T - R_{zn}), \quad (2)$$

is the phase delay between the upper and lower edges of the folds. Here,  $Q_p$  is the phase quotient [30] and  $R_{zn}$  is the nodal point ratio which specifies the pivot point of vocal fold rotation relative to the vocal fold thickness  $T$  [34]. Since symmetrical, the vocal folds collide on the glottal midline, resulting in the displacement function:

$$\xi(y, z, t) = \begin{cases} \tilde{\xi}(y, z, t) & \text{if } \tilde{\xi}(y, z, t) > 0, \\ 0 & \text{else.} \end{cases} \quad (3)$$

The glottal opening is then given by the minimum displacement along the depth,

$$\xi_{\min}(y, t) = \min_z \xi(y, z, t), \quad (4)$$

which leads to the glottal area:

$$a(t) = 2 \int_0^L \xi_{\min}(y, t) dy. \quad (5)$$

The subharmonics are introduced to the glottal vibration via  $r(t; \varphi)$ . There are two types of subharmonic glottal vibrations or a combination thereof. First is the modulation [39, 40, 41], where the entire glottis exhibit subharmonic oscillatory behavior. Second is entrained biphonation [39, 42, 43, 41], where two parts of the glottis (e.g., left and right vocal fold, or anterior and posterior regions) vibrate with different fundamental frequencies but their ratio is rational. The dataset in this study only comprises the subharmonic modulation with symmetrical vocal folds, leaving the inclusion of subharmonic biphonations for future studies. The modulation effect is implemented by a combination of amplitude modulation (AM) and frequency modulation (FM), and subharmonic reference vibration with period  $M \in \mathbb{I}$ ,  $M > 1$ , takes the form:

$$r_M(t; \varphi) = \left[ 1 + \epsilon_{AM} \sin \left( \frac{\phi(t; \varphi)}{M} + \phi_{AM} \right) \right] \times \sin \left[ \phi(t; \varphi) + \epsilon_{FM} M \sin \left( \frac{\phi(t; \varphi)}{M} + \phi_{FM} \right) \right], \quad (6)$$

where

$$\phi(t; \varphi) = 2\pi f_o t - \varphi, \quad (7)$$

$f_o$  is the speaking fundamental frequency,  $\epsilon_{AM}$  is the AM extent,  $\phi_{AM}$  is the AM phase,  $\epsilon_{FM}$  is the FM extent, and  $\phi_{FM}$  is the FM phase. Including the normal mode, we have

$$r(t; \varphi) = \begin{cases} \sin \phi(t; \varphi) & \text{if } M = 1, \\ r_M(t; \varphi) & \text{if } M > 1. \end{cases} \quad (8)$$

Here,  $\sin \phi(t; \varphi)$  is the reference vibration used in the original model [30]. The AM and FM extents generalize those of the period-doubling case [14, 29]:

$$\epsilon_{AM} = \frac{A_{\max} - A_{\min}}{A_{\max} + A_{\min}} \quad (9)$$

and

$$\epsilon_{FM} = \frac{T_{\max} - T_{\min}}{T_{\max} + T_{\min}}, \quad (10)$$

where  $A_{\max}$  and  $A_{\min}$  are the extrema of the local maxima over both  $t$  and  $\phi_{AM}$  while  $T_{\max}$  and  $T_{\min}$  are the extrema of cycle periods over both  $t$  and  $\phi_{FM}$ .

The prephonatory position  $\xi_0$  of the vocal folds is defined by [31]

$$\xi_0(y, z) = \left[ Q_a + \left( Q_s - 4Q_b \frac{z}{T} \right) \left( 1 - \frac{z}{T} \right) \right] \left( 1 - \frac{y}{L} \right), \quad (11)$$

where  $Q_a$  is the abduction coefficient,  $Q_s$  is the shape coefficient, and  $Q_b$  is the bulging quotient.

The glottal area vibration in Eq. (5) is coupled to the propagations of incidental pressure waves as depicted in Fig. 2. The model consists of five blocks: lung, subglottal tract, glottis, supraglottal tract, and lip radiation. Each block receives a forward incidental pressure wave  $f_1(t)$  from below and a backward wave  $b_2(t)$  from above and produces a forward wave  $f_2(t)$  to above and backward wave  $b_1(t)$  to below.

The subglottal and supraglottal vocal tracts are crudely modeled as leaky uniform tubes with crosssectional areas  $A_s$  and  $A_e$ , respectively. Given a tract length  $L_T$ , propagated incidental pressure waves are given by

$$\begin{aligned} f_2(t) &= \alpha^{L_T} f_1(t - cL_T) \text{ and} \\ b_1(t) &= \alpha^{L_T} b_2(t - cL_T), \end{aligned} \quad (12)$$

where  $\alpha < 1$  is the propagation gain per unit length, and  $c$  is the speed of sound.

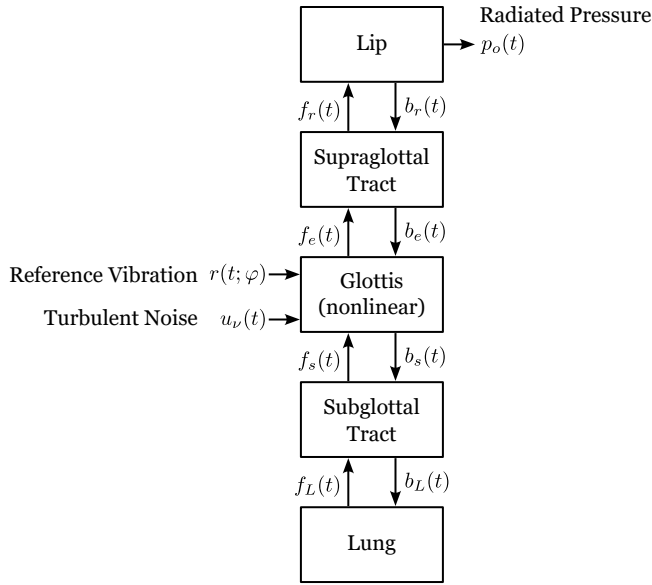


Fig. 2: Block diagram of the transmission-line voice synthesis model.

At the glottis, the glottal flow  $u(t)$  is dictated by the glottal area  $a(t)$  in Eq. (5) and the subglottal forward pressure  $f_s(t)$  and supraglottal backward pressure  $b_e(t)$  [30]:

$$u(t) = \frac{a(t)c}{1 - k_e(t)} \left\{ -\frac{a(t)}{A^*} \pm \left[ \left( \frac{a(t)}{A^*} \right)^2 + \frac{4(1 - k_e(t))}{c^2 \rho} (f_s(t) - b_e(t)) \right]^{\frac{1}{2}} \right\}, \quad (13)$$

where  $A^* = (A_e^{-1} + A_s^{-1})^{-1}$  is the effective vocal tract area,  $\rho$  is the density of the air, and the pressure recovery coefficient [44],

$$k_e(t) = 2 \frac{a(t)}{A_e} \left( 1 - \frac{a(t)}{A_e} \right). \quad (14)$$

In Eq. (13), the plus sign is used when the second term in the square brackets is negative, and vice versa.

In addition to  $r(t; \varphi)$ , the turbulent noise  $u_\nu(t)$  is another input to glottis. The noise generation follows a mixture of the noise source of the Klatt voice simulator [45] and the noise level switching mechanism based on Reynolds number [34]. It intends to model the aspiration noise during high flow rate (i.e., most open phase of vocal fold vibration) as well as the low-level noise caused by dc flow [46]:

$$u_\nu(t) = \begin{cases} \nu(t) & \text{for } Re > Re_c \\ \delta \nu(t) & \text{for } Re \leq Re_c, \end{cases} \quad (15)$$

where  $\nu(t)$  is the common noise source,

$$Re = \frac{u(t)\rho}{L\mu} \quad (16)$$

is the Reynolds number,  $Re_c = 1200$  is the critical Reynolds number, and  $\delta$  is a coefficient to suppress the noise level in the subcritical region. The noise  $\nu(t)$  is modeled as a first-order

lowpass Gaussian noise with  $-20$  dB rolloff and dc power spectral density level  $S_\nu(0)$ . Combining Eq. (13) and Eq. (15), the total glottal flow is given by

$$u_g(t) = u(t) + u_\nu(t), \quad (17)$$

and the incidental pressure wave outputs:

$$b_e(t) = f_e(t) - \frac{\rho c}{A_e} u_g(t), \quad (18)$$

and

$$f_s(t) = b_s(t) + \frac{\rho c}{A_s} u_g(t). \quad (19)$$

The lung drives the model with a constant pressure  $P_L$ , and its boundary condition is modeled by

$$f_L(t) = 0.9P_L - 0.8b_L(t). \quad (20)$$

This approximately matches the lung and subglottal tract impedances. The lip radiation  $p_o(t)$  is modeled by a circular piston in an infinite baffle [32, 37]:

$$\begin{bmatrix} P_o(s) \\ B_r(s) \end{bmatrix} = \begin{bmatrix} 2Z_r(s) \\ Z_r(s) - 1 \end{bmatrix} [Z_r(s) + 1]^{-1} F_r(s), \quad (21)$$

where  $P_o(s)$ ,  $B_r(s)$ , and  $F_r(s)$  are the Laplace transforms of  $p_o(t)$ ,  $b_r(t)$ , and  $f_r(t)$ , respectively, and

$$Z_r(s) = \frac{sL_r R_r}{R_r + sL_r} \quad (22)$$

is the lip impedance with  $L_r = 8/(3\pi c)\sqrt{A_e/\pi}$  and  $R_r = 128/(9\pi^2)$ .

To run the synthesis, the model was discretized both in time and space. The vocal fold surface is sampled to have 21 cells along the  $y$  axis and 15 cells along the  $z$  axis. The sampling rate of the simulation is  $f_s = 44100$  S/s, which also quantizes the possible vocal tract lengths to integer multiples of  $c/f_s = 0.794$  cm. The lip radiation model is converted to a discrete-time model by the bilinear transformation.

All the free parameters of the synthesis are listed in Table I. Except for  $M$ , all 21 other parameters were randomly generated during the Monte Carlo simulation. They were drawn from independent uniform distributions with the value ranges as specified on the table. Each synthesized data was generated for 1.1 seconds with fixed parameter values, thereby simulating sustained vowel-like signal. The generated signal was then resampled down to 8000 S/s, and the first 0.1 seconds (800 samples) were purged to keep only the steady-state portion of the signal. Finally, the signal was normalized by its mean and variance.

#### IV. TRAINING AND EVALUATION WITH SYNTHESIZED DATASET

To train the FCNs, 8000 1-second signals for each sub-harmonic period target  $M \in \mathcal{M}$  were generated for training (32000 total) and another 2000 each for validation (8000 total). Both models are trained using gradient descent with the Adam optimizer [47] with mini-batches composed of 32 signals selected from the training dataset in a random order. The learning rate of 0.0002 was used. An input dropout layer was inserted during training with 20% dropout rate. The

Table I: Synthesis Parameters

Block/Signal	Parameter	Range	Units	Description
$r(t; \varphi)$	$M$	{1, 2, 3, 4}		Subharmonic period
	$f_o$	[100, 300),	Hz	Speaking fundamental frequency
	$\epsilon_{AM}$	[0.1, 1.0)		AM extent (log-uniform)
	$\epsilon_{FM}$	[0.005, 0.1)		FM extent (log-uniform)
	$\phi_{AM}$	$[-\pi/2, \pi/2)$	rad	AM phase
	$\phi_{FM}$	$[-\pi/2, \pi/2)$	rad	FM phase
$u_\nu(t)$	$S_\nu(0)$	[100, 2500)	(cm <sup>3</sup> /s) <sup>2</sup> /Hz	DC psd level of full aspiration noise
	$\delta$	[0.2, 0.6)		Power reduction factor during subcritical phase
Glottis	$L$	[0.738, 1.562)	cm	Vibrating vocal fold length
	$T$	[0.18, 0.33)	cm	Vibrating vocal fold thickness
	$\xi_m$	[0.09, 0.132)	cm	Maximum glottal half width
	$Q_a$	[0.27, 0.33)		Abduction quotient
	$Q_s$	[1.8, 2.2)		Shape quotient
	$Q_b$	$[0.45Q_s, 0.55Q_s)$		Bulging quotient (relative to $Q_s$ )
	$Q_p$	[0.18, 0.22)		Phase quotient
	$R_{zn}$	[0.63, 0.77)		Nodal point ratio
	$\alpha$	[0.9983, 0.9985)	1/cm	Common propagation gain per length
Supraglottal Tract	$L_T$	[11.111, 15.873)	cm	Supraglottal tract length
	$A_e$	[1.0, 5.0)	cm <sup>2</sup>	Supraglottal tract area
Subglottal Tract	$L_T$	[6.349, 9.524)	cm	Subglottal tract length
	$A_s$	[1.0, 3.0)	cm <sup>2</sup>	Subglottal tract area
Lung	$P_L$	[7056, 8624)	dyn/cm <sup>2</sup>	Lung pressure

training persisted over 20 epochs and the coefficients with the best validation accuracy was chosen. All the snapshots of every signal were used in the training to capture all the possible phases of the periodic signal. Due to the different window sizes, FCN-401 and FCN-785 have different numbers of snapshots per signal: 478 for FCN-401 and 454 for FCN-785.

To evaluate the trained networks, another 4000 signals were generated. For these,  $f_o$  and the SHR were recorded along with  $M$ . The SHR was estimated from the periodogram  $S(f)$  of the signal with Hamming window by

$$SHR = \frac{\sum_{k \in \mathcal{K}_s} S(kf_o/M)}{\sum_{k \in \mathcal{K}_h} S(kf_o/M)}, \quad (23)$$

where  $\mathcal{K}_h$  is a set of the  $f_o$ -harmonic multipliers under 4 kHz, and  $\mathcal{K}_s$  is a set of the subharmonic multipliers. Given the  $k$ th output of an FCN,  $\{P_{M,k} : M \in \mathcal{M}\}$ , its subharmonic period is estimated by  $\hat{M}_k = \operatorname{argmax}_{M \in \mathcal{M}} P_{M,k}$ .

The overall classification accuracy of FCN-401 is 98.1% and that of FCN-785 is 98.9%. The confusion matrices of the two FCNs are shown in Fig. 3. FCN-785 achieved above 98.5% conditional accuracies across all  $M$  with 0.5% higher results for the normal voicing detection ( $M = 1$ ). Subharmonic voicings ( $M > 1$ ) are more likely to be mistaken as normal ( $M = 1$ ) than with another subharmonic period ( $\hat{M} > 1$ ). FCN-401 follows the same trend but with increased errors. Its normal voicing detection matches that of FCN-785, but the subharmonic period detections lags behind by about 0.75% or more.

FCN-401 performed noticeably worse for the  $M = 2$  signals (96.94% accuracy). In contrast, FCN-785 maintained a similar accuracy across all subharmonic periods. The observed performance loss by FCN-401 for  $M = 2$  likely stems from two reasons: SHR imbalance across  $M$  and short window size. The SHRs of the acoustic signals are not identical as shown in Fig. 4(a) although the identical distributions were used for AM

		(a) FCN-401			
True subharmonic period, $M$	1	99.55%	0.32%	0.12%	0.01%
	2	3.01%	96.94%	0.03%	0.02%
	3	1.46%	0.26%	97.93%	0.36%
	4	1.29%	0.23%	0.54%	97.94%
		Detected subharmonic period, $\hat{M}$	1	2	3
		(b) FCN-785			
True subharmonic period, $M$	1	99.30%	0.56%	0.14%	0.01%
	2	1.06%	98.87%	0.04%	0.03%
	3	0.89%	0.23%	98.68%	0.21%
	4	0.74%	0.10%	0.23%	98.93%
		Detected subharmonic period, $\hat{M}$	1	2	3

Fig. 3: Synthetic classification confusion matrices: (a) FCN-401, (b) FCN-785.

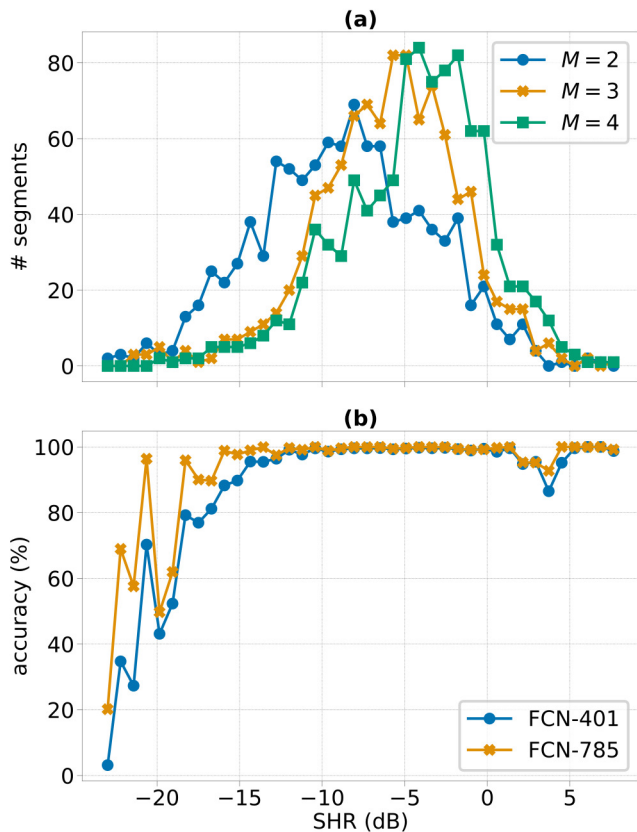


Fig. 4: Synthetic classification performance vs. SHR ( $M > 1$  signals only): (a) SHR distribution and (b) classification accuracy vs. SHR.

and FM extents across all  $M$ . The expected SHR of  $M = 2$  is lower than  $M > 2$  signals, and the presence of the  $M > 2$  signals with SHR below  $-10$  dB rapidly declines. This likely deemphasized the importance of the low SHR range during the training, resulting in poor accuracy as shown in Fig. 4(b). A compounding factor is that lower the SHR the harder to detect the subharmonics. Fig. 4(b) also displays that the subharmonic detection performs better with a longer analysis window.

Another effect which separated FCN-785 from FCN-401 is  $f_o$  as shown in Fig. 5. There is a clear performance gap between the two FCNs at lower  $f_o$  range. Although FCNs do not strictly follow the rules of traditional spectral analysis, a form of spectral resolution seems to be playing a role here. In spectral analysis, resolving two tones which are separated by 50 Hz (i.e., tones of the  $M = 2$  signals at 100 Hz) requires a snapshot size of at least 40 ms (320 samples) under noise-free condition. An even longer snapshot is needed for the low-SHR signals as the subharmonic tones are much weaker than the harmonic tones. FCN-401 is operating close to this limit; thus, its accuracy suffers as  $f_o$  reduces. FCN-785, on the other hand, can maintain its accuracy across  $f_o$ .

## V. CASE STUDIES OF PATHOLOGICAL SUSTAINED VOWELS

Next, the behaviors of the trained FCNs are evaluated with sustained /a/ vowel recordings of selected pathological voices

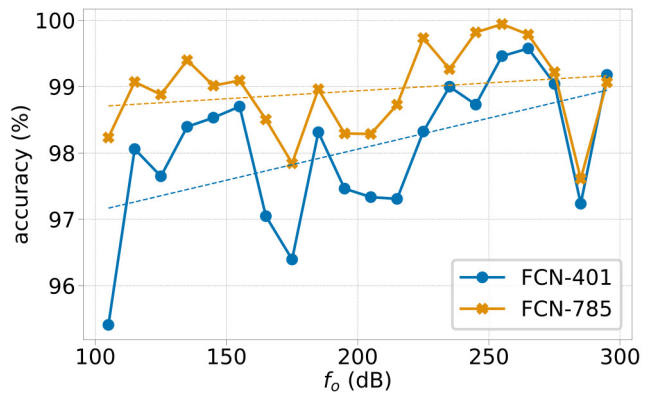


Fig. 5: Synthetic classification performance vs.  $f_o$ . Dashed lines are the least squares fitted lines.

from KayPENTAX (Massachusetts Eye and Ear Infirmary) Disordered Voice Database [48]. These recordings are sampled at 25000 S/s and each about 1 second long. The onsets and offsets of the phonations are pre-trimmed. To evaluate, the recordings are first resampled to 8000 S/s and normalized over the entire duration before input to the FCNs. The estimated subharmonic period sequence,  $\hat{M}_k = \operatorname{argmax}_{M \in \mathcal{M}} P_{M,k}$ , and the probabilities of the estimates  $P_{\hat{M}_k,k}$  are observed for both FCN-401 and FCN-785.

The first case in Fig. 6 consists of  $f_o \approx 206$  Hz phonation, starting with period-tripling subharmonics until  $t = 0.42$  s, followed by a brief period of unlocked modulation ( $< 0.63$  s) to normal phonation ( $< 0.92$  s) before the period-3 returning. Both networks estimate either  $M = 1$  or 3, except for FCN-401 occasionally reporting low-probability  $M_k = 4$  snapshots. This case exemplifies the strictness of the FCNs in detecting the subharmonics. Despite unlocked modulation was not included in the training dataset, both selected  $M = 1$  rather than visually viable  $M = 2$ . Also, consistent near-1.0 probabilities of  $M = 3$  cases were obtained only between 0.1 and 0.2 s, possibly indicating a weaker lock. Finally, this case demonstrates the tradeoff of FCN-785. While its longer window size provides better estimation performance than FCN-401, it also negatively impact the ability to detect the transition point. At  $t = 0.4$ , it leaves  $M_k = 3$  slightly earlier than when it occurs in the spectrogram and FCN-401 results.

The second case in Fig. 7 demonstrates the outputs of the trained FCNs when the input signal contains suspected biphonation, which is apparent until  $t = 0.75$  s. The biphonation is suspected because the traces of two dominant low-frequency tones are consistently present, each likely representing the first harmonic of its periodic vibration. At the beginning,  $f_{o,1} = 154$  Hz and  $f_{o,2} = 231$  Hz, which constitute a 2 : 3 subharmonic arrangement. Then, biphonation continues to exist through what appears to be less stable segment between 0.44 and 0.75 s. While we can continue to observe the two first harmonics, whether they are locked or not is no longer prevalent to naked eyes. Although the FCNs are not trained for this type of subharmonics, both FCNs

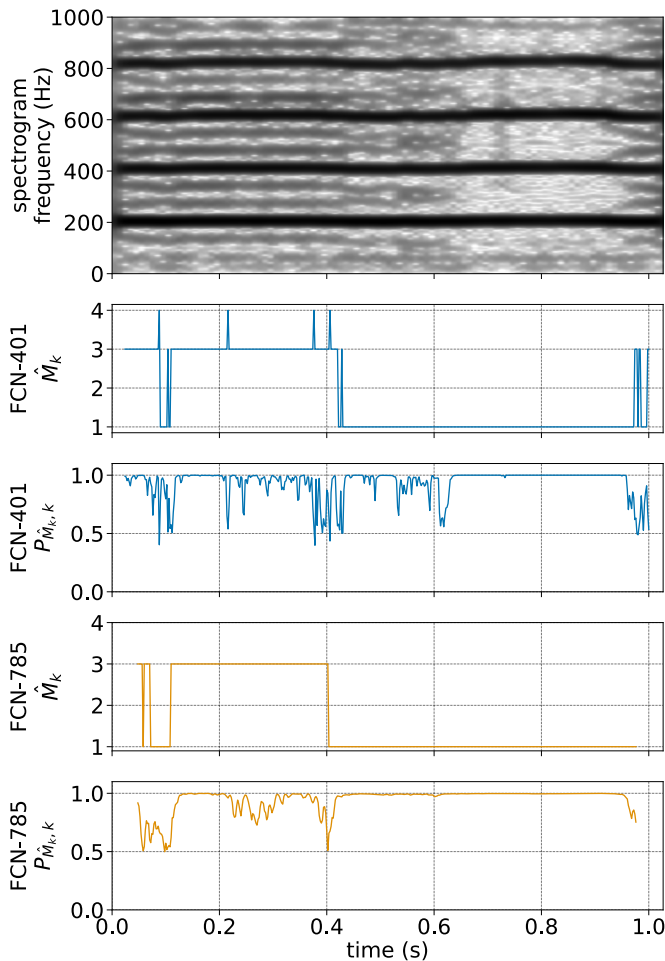


Fig. 6: Case Study 1 (modulation): Spectrogram and outputs of trained FCNs—estimated subharmonic periods  $\hat{M}_K$  and their probabilities  $P_{\hat{M},k}$ .

suggest that there are moments of locked oscillation with high confidence. FCN-785 often estimates  $\hat{M}_k = 4$  over sustained periods in the unstable segment. Together, it appears that we have 3:4 in the first half and 4:5 in the second half. This is an encouraging results, demonstrating the robustness of the FCN-based subharmonic detection. The subharmonics due to biphonation has a different spectral construct than those due to the modulation, but high confident estimates are obtained despite the training dataset only contains modulation signals only. FCNs would likely perform better if the subharmonic biphonation cases are included in the training data.

The final case in Fig. 8 illustrates the behaviors of the trained FCNs for a signal with severe vocal tremor, which includes  $f_o$  tremor with the period of 4 s and peak-to-peak extent of 35 Hz. Neither FCNs consistently estimated  $\hat{M}_k = 1$  during the short segments of clean harmonics ( $t$ : 0.05-0.13 and 0.77-0.84). FCN-401's inability to maintain  $\hat{M}_k = 1$  for the entirety of these segments is likely due to its training dataset only consists of fixed  $f_o$ . FCN-785, which does not register  $\hat{M}_k = 1$  at all, is further penalized by the shortness of these segments coupled with the homogeneous training dataset. This indicates that the training data must include  $f_o$  variability (e.g.,

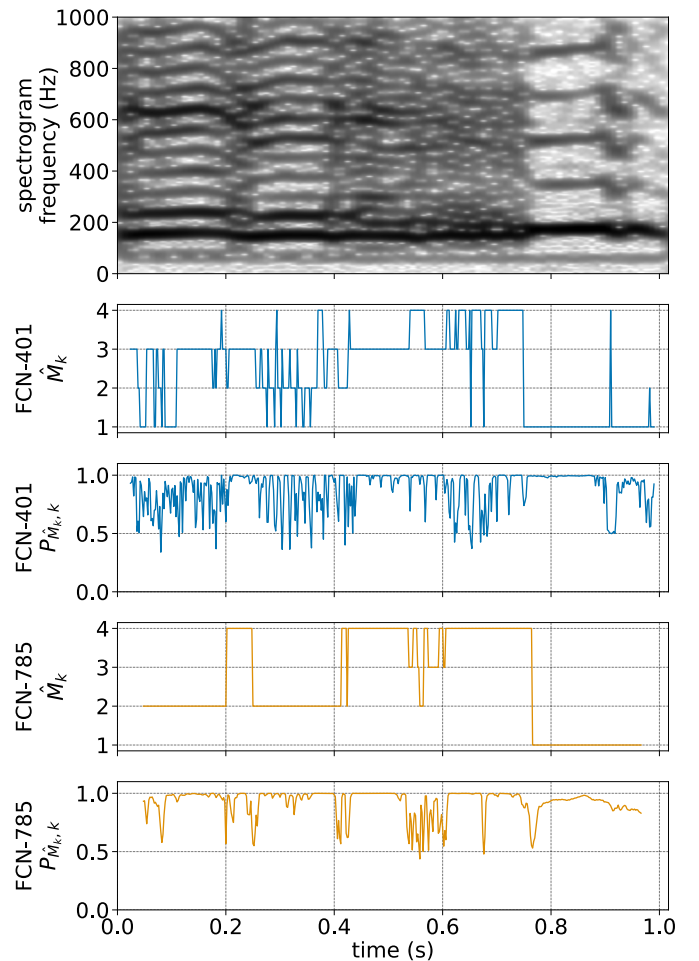


Fig. 7: Case Study 2 (suspected biphonia): Spectrogram and outputs of trained FCNs—estimated subharmonic periods  $\hat{M}_K$  and their probabilities  $P_{\hat{M},k}$ .

the flutter effect of the Klatt synthesizer [45]) to improve the performance. This is also crucial to extend the use to connected speech, in which  $f_o$  constantly fluctuates.

## VI. CONCLUSIONS

The synthetic evaluation indicates that the proposed FCNs are highly capable of correctly identifying the subharmonic periods. Testing with pathological voice recordings further supports indicates that the FCNs' potential to identify subharmonic modulations despite being trained with a crude vocal tract model and arbitrarily selected parameter ranges. This also demonstrates the FCNs' ability to ignore weak unlocked modulation. The testing also revealed a number of remaining challenges to be fulfilled. First, the pathological voice simulation needs to be extended to account for additional pathological behaviors like subharmonic biphonation, intermittency, and variation in fundamental frequency. Second, a better stochastic representation of human voice production system is crucial to refine the synthesis parameter ranges. These will yield improved training dataset, and subsequent tuning of the FCN architecture and hyperparameters will likely result in a dependable subharmonic detector.

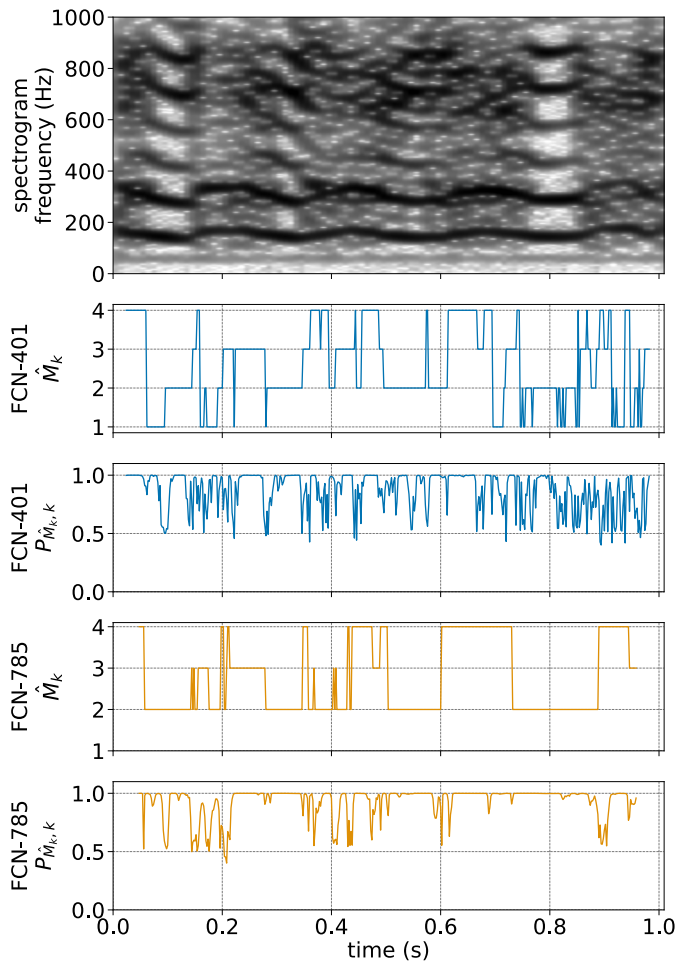


Fig. 8: Case Study 3 (severe vocal tremor): Spectrogram and outputs of trained FCNs—estimated subharmonic periods  $\hat{M}_K$  and their probabilities  $P_{\hat{M},k}$ .

#### REFERENCES

- [1] A. Behrman, C. J. Agresti, E. Blumstein, and N. Lee, “Microphone and electroglottographic data from dysphonic patients: Type 1, 2 and 3 signals,” *J. Voice*, vol. 12, no. 2, pp. 249–260, Jan. 1998.
- [2] L. Cavalli and A. Hirson, “Diplophonia reappraised,” *J. Voice*, vol. 13, no. 4, pp. 542–556, 1999.
- [3] F. Núñez Batalla, C. Suárez Nieto, C. Muñoz Pinto, L. Baragaño Río, M. J. Alvarez Zapico, and A. Martínez Ferreras, “[Spectrographic study of voice disorders: subharmonics],” *Acta Otorrinolaringol. Esp.*, vol. 51, no. 1, pp. 52–56, 2000.
- [4] E. Kramer, R. Linder, and R. Schönweiler, “A study of subharmonics in connected speech material,” *J. Voice*, vol. 27, no. 1, pp. 29–38, Jan. 2013.
- [5] T. Ikuma, A. J. McWhorter, L. Adkins, and M. Kunduk, “Investigation of vocal bifurcations and voice patterns induced by asymmetry of pathological vocal folds,” *J. Speech Lang. Hear. Res.*, vol. 66, no. 1, pp. 48–60, Jan. 2023.
- [6] H. Hollien, P. Moore, R. W. Wendahl, and J. F. Michel, “On the nature of vocal fry,” *J. Speech Hear. Res.*, vol. 9,

- no. 2, pp. 245–247, Jun. 1966.
- [7] C. T. Herbst, S. Hertegard, D. Zangger-Borch, and P.-Å. Lindestad, “Freddie Mercury—acoustic analysis of speaking fundamental frequency, vibrato, and subharmonics,” *Logoped. Phoniatr. Vocol.*, vol. 42, no. 1, pp. 29–38, Jan. 2017.
- [8] K. Omori, H. Kojima, R. Kakani, D. H. Slavitt, and S. M. Blaugrund, “Acoustic characteristics of rough voice: Subharmonics,” *J. Voice*, vol. 11, no. 1, pp. 40–47, Mar. 1997.
- [9] C. C. Bergan and I. R. Titze, “Perception of pitch and roughness in vocal signals with subharmonics,” *J. Voice*, vol. 15, no. 2, pp. 165–175, Jun. 2001.
- [10] X. Sun and Y. Xu, “Perceived pitch of synthesized voice with alternate cycles,” *J. Voice*, vol. 16, no. 4, pp. 443–459, Dec. 2002.
- [11] Y. Huang, “Perception and imitation of period-doubled phonation: Pitch and voice quality,” *J. Acoust. Soc. Am.*, vol. 156, no. 2, pp. 1391–1412, Aug. 2024.
- [12] T. Ikuma, A. J. McWhorter, and M. Kunduk, “Evaluation of machine-learning pitch estimation algorithms,” in *13th ICVPB*, Erlangen, Germany, Jul. 2024, pp. 28–9. [Online]. Available: [https://www.icvpb-2024.de/documents/8/Program\\_ICVPB2024.pdf](https://www.icvpb-2024.de/documents/8/Program_ICVPB2024.pdf)
- [13] T. Ikuma, M. Kunduk, and A. J. McWhorter, “Comparison of fundamental frequency estimators with subharmonic voice signals,” 2025, arXiv preprint, <https://arxiv.org/abs/2501.04789>.
- [14] I. R. Titze, *Workshop on Acoustic Voice Analysis: Summary Statement*. Denver, CO, USA: National Center for Voice and Speech, 1994. [Online]. Available: [ncvs.org/archive/freebooks/summary-statement.pdf](https://ncvs.org/archive/freebooks/summary-statement.pdf)
- [15] KayPENTAX, “Multi-Dimensional Voice Program (MDVP) model 5105 software instruction manual,” Jun. 2008.
- [16] D. Deliyski, “Acoustic model and evaluation of pathological voice production,” in *Eurospeech 1993*, Berlin, Germany, 1993, pp. 969–1972.
- [17] X. Sun, “A pitch determination algorithm based on subharmonic-to-harmonic ratio,” in *Proc. 6th ICSLP*, vol. 4, Beijing, China, 2000, pp. 676–679.
- [18] J. Hlavnička, R. Čmejla, J. Klempř, E. Růžička, and J. Rusz, “Acoustic tracking of pitch, modal, and subharmonic vibrations of vocal folds in Parkinson’s Disease and Parkinsonism,” *IEEE Access*, vol. 7, pp. 150 339–150 354, 2019.
- [19] P. Aichinger, M. Hagmüller, I. Roesner, B. Schneider-Stickler, J. Schoentgen, and F. Pernkopf, “Fundamental frequency tracking in diplophonic voices,” *Biomed. Signal Process. Control*, vol. 37, pp. 69–81, Aug. 2017.
- [20] P. Aichinger, M. Hagmüller, B. Schneider-Stickler, J. Schoentgen, and F. Pernkopf, “Tracking of multiple fundamental frequencies in diplophonic voices,” *IEEE/ACM Trans. Audio Speech Lang. Process.*, vol. 26, no. 2, pp. 330–341, Feb. 2018.
- [21] S. N. Awan and J. A. Awan, “A two-stage cepstral analysis procedure for the classification of rough voices,” *J. Voice*, vol. 34, no. 1, pp. 9–19, Jan. 2020.



- [22] I. Kitayama, K. Hosokawa, S. Iwaki, M. Yoshida, A. Miyauchi, M. Ogawa, and H. Inohara, "Validation of subharmonics quantification using two-stage cepstral analysis," *J. Voice*, p. S0892199723003892, Dec. 2023.
- [23] L. Ardaillon and A. Roebel, "Fully-convolutional network for pitch estimation of speech signals," in *Inter-speech 2019*, Sep. 2019, pp. 2005–2009.
- [24] J. W. Kim, J. Salamon, P. Li, and J. P. Bello, "Crepe: A convolutional representation for pitch estimation," in *IEEE ICASSP 2018*, Calgary, AB, Apr. 2018, pp. 161–165.
- [25] J. Long, E. Shelhamer, and T. Darrell, "Fully convolutional networks for semantic segmentation," in *Proc IEEE CVPR 2015*. Boston, MA, USA: IEEE, Jun. 2015, pp. 3431–3440.
- [26] Z. Wang, W. Yan, and T. Oates, "Time series classification from scratch with deep neural networks: A strong baseline," in *Proc. IJCNN 2017*. Anchorage, AK, USA: IEEE, May 2017, pp. 1578–1585.
- [27] H. Ismail Fawaz, G. Forestier, J. Weber, L. Idoumghar, and P.-A. Muller, "Deep learning for time series classification: A review," *Data Min. Knowl. Discov.*, vol. 33, no. 4, pp. 917–963, Jul. 2019.
- [28] P. Dejonckere and J. Lebacqz, "An analysis of the diphonia phenomenon," *Speech Commun.*, vol. 2, no. 1, pp. 47–56, May 1983.
- [29] C. T. Herbst, "Performance evaluation of subharmonic-to-harmonic ratio (SHR) computation," *J. Voice*, vol. 35, no. 3, pp. 365–375, May 2021.
- [30] I. R. Titze, "Parameterization of the glottal area, glottal flow, and vocal fold contact area," *J. Acoust. Soc. Am.*, vol. 75, no. 2, pp. 570–580, 1984.
- [31] —, "A four-parameter model of the glottis and vocal fold contact area," *Speech Commun.*, vol. 8, no. 3, pp. 191–201, Sep. 1989.
- [32] B. Story, "Physiologically-Based Speech Simulation Using an Enhanced Wave-Reflection Model of the Vocal Tract," Ph.D. dissertation, University of Iowa, Iowa City, IA, May 1995.
- [33] J. Liljencrants, "Speech Synthesis with Reflection-Type Line Analog," Ph.D. dissertation, Royal Institute of Technology, Stockholm, Sweden, 1985.
- [34] R. A. Samlan and B. H. Story, "Relation of structural and vibratory kinematics of the vocal folds to two acoustic measures of breathy voice based on computational modeling," *J. Speech Lang. Hear. Res.*, vol. 54, no. 5, pp. 1267–1283, Oct. 2011.
- [35] R. A. Samlan, B. H. Story, and K. Bunton, "Relation of perceived breathiness to laryngeal kinematics and acoustic measures based on computational modeling," *J. Speech Lang. Hear. Res.*, vol. 56, no. 4, pp. 1209–1223, Aug. 2013.
- [36] R. A. Samlan, B. H. Story, A. J. Lotto, and K. Bunton, "Acoustic and perceptual effects of left–right laryngeal asymmetries based on computational modeling," *J. Speech Lang. Hear. Res.*, vol. 57, no. 5, pp. 1619–1637, Oct. 2014.
- [37] K. Ishizaka and J. L. Flanagan, "Synthesis of voiced sounds from a two-mass model of the vocal cords," *Bell Syst. Tech. J.*, vol. 51, no. 6, pp. 1233–1268, 1972.
- [38] I. R. Titze, "The physics of small-amplitude oscillation of the vocal folds," *J. Acoust. Soc. Am.*, vol. 83, no. 4, pp. 1536–1552, 1988.
- [39] S. Kiritani, H. Hirose, and H. Imagawa, "High-speed digital image analysis of vocal cord vibration in diphonia," *Speech Commun.*, vol. 13, no. 1-2, pp. 23–32, 1993.
- [40] S. Kniesburges, A. Lodermeier, S. Becker, M. Traxdorf, and M. Döllinger, "The mechanisms of subharmonic tone generation in a synthetic larynx model," *J. Acoust. Soc. Am.*, vol. 139, no. 6, pp. 3182–3192, Jun. 2016.
- [41] T. Ikuma, M. Kunduk, D. Fink, and A. J. McWhorter, "Synthetic multi-line kymographic analysis: A spatiotemporal data reduction technique for high-speed videodendoscopy," *J. Acoust. Soc. Am.*, vol. 140, no. 4, pp. 2703–2713, Oct. 2016.
- [42] P. Mergell, H. Herzel, and I. R. Titze, "Irregular vocal-fold vibration—High-speed observation and modeling," *J. Acoust. Soc. Am.*, vol. 108, no. 6, pp. 2996–3002, 2000.
- [43] J. Neubauer, P. Mergell, U. Eysholdt, and H. Herzel, "Spatio-temporal analysis of irregular vocal fold oscillations: Biphonation due to desynchronization of spatial modes," *J. Acoust. Soc. Am.*, vol. 110, no. 6, pp. 3179–3192, 2001.
- [44] I. R. Titze, "Regulating glottal airflow in phonation: Application of the maximum power transfer theorem to a low dimensional phonation model," *J. Acoust. Soc. Am.*, vol. 111, no. 1, pp. 367–376, Jan. 2002.
- [45] D. H. Klatt and L. C. Klatt, "Analysis, synthesis, and perception of voice quality variations among female and male talkers," *J. Acoust. Soc. Am.*, vol. 87, no. 2, pp. 820–857, 1990.
- [46] E. B. Holmberg, R. E. Hillman, and J. S. Perkell, "Glottal airflow and transglottal air pressure measurements for male and female speakers in soft, normal, and loud voice," *J. Acoust. Soc. Am.*, vol. 84, no. 2, pp. 511–529, Aug. 1988.
- [47] D. P. Kingma and J. Ba, "Adam: A Method for Stochastic Optimization," in *ICLR 2015*. San Diego, CA: arXiv, 2015.
- [48] KayPENTAX and Massachusetts Eye and Ear Infirmary, "Disordered Voice Database and Program [Model 4337]," 2006.